Egypt. J. Chem. **Vol. 65,** No. 1, pp. 481 - 488 (2022)

Egyptian Journal of Chemistry

http://ejchem.journals.ekb.eg/

Facile Synthesis of Spinel $CoCr_2O_4$ and Its Nanocomposite with ZrO_2: Employing in Photo-catalytic Decolorization of Fe (II)-(luminol-Tyrosine) Complex

Hamad Hamid Kazem[1], Luma Majeed Ahmed[1*] and Mohanad Mousa Kareem[2]

[1] Department of Chemistry, College of Science, University of Kerbala, Kerbala, Iraq
[2] Department of Chemistry, College of Science, University of Babylon, Babylon, Iraq

Abstract

In this project, the deep green power from spinel cobalt chromite ($CoCr_2O_4$) nano-crystals carried out using the co-precipitation method and then calcinated at 600 ºC for 4 hours. This produced nano-crystal (spinel $CoCr_2O_4$) fabricated using the ultrasonic technique to link it with zirconium dioxide (ZrO_2) in ratios 1:2 and 1:3, respectively. The X-ray diffraction (XRD), scan electron microscopy (SEM), and energy-dispersive X-rays (EDX), as well as ultraviolet-visible spectrophotometry used to describe the characterizations of prepared materials. The XRD analysis demonstrated that the spinel $CoCr_2O_4$ synthesis and their composites were found to be nanoparticles. XRD spectra indicated that the spinel $CoCr_2O_4$ is successfully loaded on ZrO_2, because, the 2θ of ZrO_2 is shifted toward a high 2θ value after spinel $CoCr_2O_4$ loaded. This case is attituded to the tiny Co^{2+} and Cr^{3+} ions combined with Zr^{4+} in crystal lattice. The SEM images and EDX spectra of these obtained nanomaterials were found to be spherical agglomerations with an enhanced degree of surface roughness after surface fabrication. On the other side, the bandgap of spinel $CoCr_2O_4$ nanocrystals elevated from 3.2 to 4.8 eV with increasing the ZrO_2 dose. Under UV-A light, the photocatalytic decolorization efficiency of Fe (II)-(luminol-Tyrosine) complex utilizing spinel $CoCr_2O_4$ nanocrystals was tested, and it increases from 17.57 % to 30.67% and 41.97% when its nanocomposite was used in 1:2 and 1:3 ratios, respectively. The elevated efficiency after modified the spinel $CoCr_2O_4$ surface with ZrO_2 as nanocomposite, due to increasing the acidity of the spinel $CoCr_2O_4$ surface that enhances the adsorption of hydroxyl on its surface then generality of the hydroxyl radical, and reducing the recombination. The photoreaction using spinel $CoCr_2O_4$ nanocrystals, ZrO_2, and their composites were followed pseudo-first-order kinetics depended on the complex concentration.

Keywords: Spinel $CoCr_2O_4$; Spinel $CoCr_2O_4$ / ZrO_2 nanocomposite; Co-precipitation; Facile Synthesis; Photo-catalytic decolorization; and Fe(II)-(luminol-Tyrosine) complex.

1.Introduction

Many researchers who worked in the nanoscience and nanotechnology field, and found the basic science and technical breakthroughs abound in this field. In the last several decades, many novel materials with dimensions in the nanoscale were synthesized and characterized, which including nanoparticles, nanobelts, like-flower nanostructure, nanowires, Quasi-spherical nanoparticle, and nanotubes, were prepared[1-٦]. Though the design and synthesis of nanoscale materials with controllable qualities is a continuous difficulty in the area of nanoscience and nanotechnology, however, it remains important materials, that have good electrical, optical, and physical characteristics[7]. The use of nanotechnology in wastewater treatment that is produced by scientific labs or industry can make the wastewater treatment is better[8-12]. Spinel $CoCr_2O_4$ nanomaterial is a distinctive material that has a low bandgap, used as a pigment to colorant of ceramic, porcelain, plastic, and solar absorber coatings. Moreover, the conventional spinel cubic structure shows up with two kinds of cation sublattice. In the A sub-lattice, there are Co^{2+} ions that occupy the tetrahedral (A) sites, and in the B sub-lattice, Cr^{3+} ions are occupying the octahedral (B) sites[13-15]. Magnetic characteristics of the spinel $CoCr_2O_4$ greatly rely on the number of cations that are grouped at sites A and B in the aAaAAaAssscxxx spinel lattice. NP-influenced magnetic characteristics also differ between single NPs and their counter bulk material[16], which is consistent with their lattice distortion, surface imperfections, and the existence of interactions between NPs. When it comes to the family of chromites, cobalt chromite nanoparticles ($CoCr_2O_4$ NPs) have become popular because of their

*Corresponding author e-mail: luma.ahmed@uokerbala.edu.iq ; (Luma M. ahmed).
Receive Date: 18 June 2021, Revise Date: 09 July 2021, Accept Date: 10 July 2021
DOI: 10.21608/EJCHEM.2021.81251.4025

multiferroic characteristics. The spinel $CoCr_2O_4$ has a cubic spinel structure with multiferroicity, and a conical spin ordering has been discovered in this material. [17]. Due to the conflicting Co-Co, Cr-Cr, and Co-Cr interactions, cobalt chromate nanoparticles undergo three sequential magnetic transitions: At temperature collinear (T_C) 95 K, the magnetic transition from paramagnetic to ferromagnetic (FIM) phase happens; at temperature non-collinear spiral (T_S) 26 K, the magnetic transition from FIM to an incommensurate conical-spiral phase happens; and at temperature long-range collinear (T_L) 14 K, the magnetic transition from ferromagnetic (FIM) to an incommensurate conical-spiral phase happens [18]. Kind-II multiferroic materials, such as pristine spinel $CoCr_2O_4$ nanoceramics, are a type of material that manifests magnetoelectric coupling as well as two or more ferroic features. Storing charges in electronic memory devices are made much more efficient using these nanoceramics [19].

The goal of this work project is to focus on the facile synthesis of spinel $CoCr_2O_4$ nanocrystals using co-precipitation and then modified with ZrO_2 in 1:2 and 1:3 ratios using ultrasonic waves, to reduce the recombination and increase the surface acidity. The structural, morphological, and optical characteristics are determined to conform to this synthesis, as well as its photocatalytic characteristics, which have also been examined on a colored solution from Fe (II)-(luminol-Tyrosine) Complex.

2. Experimental

A. Materials

The powdered ore of zirconium dioxide was obtained from Riedel-De-Haen AG, Seelze, Hanover, Germany. Using cobalt nitrate hexahydrate (Co $(NO_3)_2.6H_2O$), chromium nitrate nonahydrate (Cr $(NO_3)_3.9H_2O$), and ammonia solution (25 percent) were supplied from Merck. Cetyltrimethylammonim bromide (CTAB) was supplied by Interchimiques SA. Ferrous chloride trihydrate $FeCl_2 \cdot 2H_2O$, absolute ethanol (C_2H_5OH), iron (III) sulfate hydrate ($Fe_2(SO_4)_3.H_2O$), hydrochloric acid (HCl), and sodium hydroxide (NaOH) were supplied from BDH.

The organic chemistry lab teams at the University of Babylon, college of science, department of chemistry, provided the Fe (II)-(luminol-Tyrosine) complex.

B. Synthesis of Spinel $CoCr_2O_4$ nanocrystals

Spinel $CoCr_2O_4$ nanocrystals were synthesized via the co-precipitation method. At the outset, cobalt nitrate (0.5 M) and chromium nitrate (1M) was prepared and transferred to an ultrasonic bath at 75 °C for 1 hour. In the second step, the chromium nitrate solution was put in a beaker with size 500 mL, and then cobalt nitrate solution was slowly added to chromium nitrate solution using an ultrasonic bath at 75 °C, and thrown for 1 hour. In the third step, the generated mixture was stirred and heated at the same temperature for a further two hours using a magnetic stirrer. Following that, 1% CTAB is added to the mixture as a capping agent to prevent metal hydroxide formed. 25% aqueous ammonia solution was dropwise added to the last solution until a pH makes it 9.

The produced deep green precipitate was filtered and washed with distilled water many times until the filtrate reached to pH of around 7 to ensure all contaminants are removed, and then washed with ethanol to remove the water humidity. The deep green precipitate was dried overnight in a desiccator, then calcinated for 4 hours at 600 °C.

Equations 1 and 2 were suggested the chemical reaction of spinel $CoCr_2O_4$ formed.

$$Co(NO_3)_2.6H_2O + 2Cr(NO_3)_3.9H_2O + 8NH_4OH \rightarrow Co(OH)_2.Cr(OH)_6 + 8NH_4NO_3 + 15H_2O \quad \ldots(1)$$

$$Co(OH)_2.Cr(OH)_6 \rightarrow CoO.Cr_2O_3 + 4H_2O \quad \ldots(2)$$

2.2 Synthesis of spinel $CoCr_2O_4/ZrO_2$ nanocomposite

The preceding procedures were carried out with the used ultrasonic technique to like two photocatalysts as a nanocompousite[2,3]. The 1:2 and 1:3 ratios from spinel $CoCr_2O_4$: ZrO_2 were created as nanocomposites employing an ultrasonic wave at 75 °C for 1 h. As a result, it is acceptable to provide sufficient energy to combine ZrO_2 and spinel $CoCr_2O_4$ into the crystal lattice. The spinel $CoCr_2O_4$ solution was added step by step to incorporate with ZrO_2 solution in two ratios 1:2 and 1:3 via ultrasonic bath (60 kHz) for 2 hours at 75 ºC. The generated mixture was stirred with heated at the same temperature for a further two hours using a magnetic stirrer, and then dried at a temperature of 75 °C to produce a deep green suspension from the spinel $CoCr_2O_4/ZrO_2$ nanocomposite that filtered and stored overnight in a desiccator using silica gel. The chemical equation for spinel $CoCr_2O_4/ZrO_2$ nanoparticles synthesis in different ratios was suggested using equation 3.

$$CoCr_2O_4 + ZrO_2 \longrightarrow CoCr_2O_4\text{-}ZrO_2 \quad \ldots(3)$$

2.3 Application of the Spinel $CoCr_2O_4$ and spinel $CoCr_2O_4/ZrO_2$ nanocomposites are used to decolorize Fe (II)-(luminol-Tyrosine) dye solution.

In figure 1, the photoreaction was carried out using a handmade photoreactor. This photoreactor includes 400 watts of UV-lamp power. The reactor's body is constructed from a wooden box to prevent hazardous light, which contains a magnetic stirrer, a Pyrex glass beaker (500 mL), a Teflon bar, and two various fans[20-22].

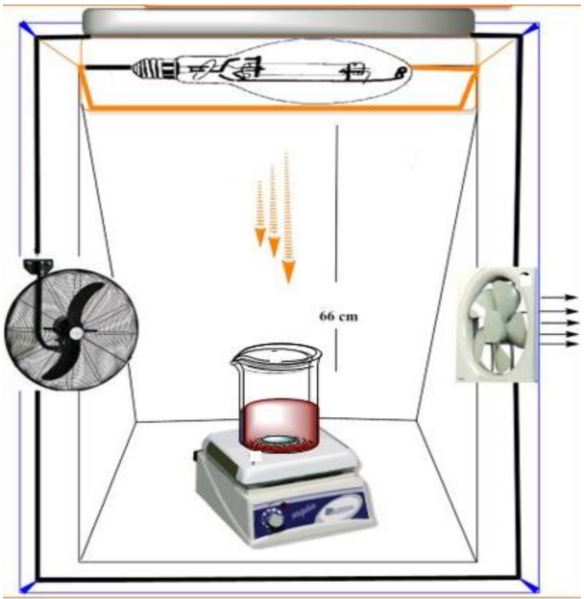

Figure 1. Diagrammatic representation of a Homemade Photocatalytic Reactor Unit.

At a temperature of 20 °C, exact 0.01g of spinel $CoCr_2O_4$ or ZrO_2 or spinel $CoCr_2O_4/ZrO_2$ nanocomposites were added to 100 ppm from Fe (II)-(luminol-Tyrosine) complex solution as a chocolate colored solution with pH 7.3 that dissolved in DMSO. Without irradiation, the suspension solution was magnetically agitated for 30 minutes to allow for the establishment of an equilibrium adsorption condition[23-27]. Following the adsorption stage, the suspension was exposed to UV light, and about 3 mL of aliquots were collected at 10-minute intervals until 40 minutes. The collected suspensions were centrifuged twice at 4000 rpm for 30 minutes, and the absorbance of the resulting filters was measured at 475 nm using a UV-Vis spectrophotometer (AA-1800, Shimadzu). Equations 4 and 5 were used to get the rate constant of this photoreaction and the efficiency of decolorization [28- 34].

$$\ln\left(\frac{C_o}{C_t}\right) = k_{app}t \quad \ldots (4)$$

$$PDE\ \% = \frac{(C_o - C_t)}{C_o} \times 100 \quad \ldots (5)$$

3.Results and Discussion

A. *Structural Properties*

According to figure 2, XRD analysis was used to determine the structure of all photocatalyst samples utilizing two angles ranging from 20° to 80° on a Lab X XRD 6000-Shimadzu.In Figure 2, XRD analysis was utilized to detect the structure and phase of spinel $COCr_2O_4$ powder and a produced spinel $CoCr_2O_4$-ZrO_2 nanocomposite. The $CoCr_2O_4$'s key diffraction peaks are located at 30.3779°, 35.8022°, 43.3839°, 57.5052°, and 63.1014° with miller indexes (220), (311), (400), (511), and (440) planes, respectively (JCPDS Card No. 00-022-1084), and are in strong agreement with findings from references [35,36]. On the other hand, the ZrO_2 peaks exist at diffraction angles (111), (200), (220), and (311) with four locations of 2θ that equal to 30.2973°, 35.0778°, 50.4580°, and 59.9693°, respectively(JCDS card No.00-049-1642) [36,37].

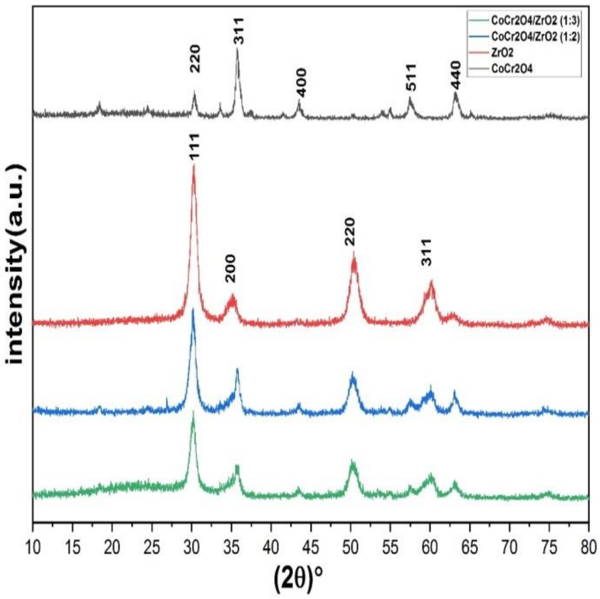

Figure 2: XRD pattern of spinel $CoCr_2O_4$, ZrO_2, spinel $CoCr_2O_4$-ZrO_2 (1:2) nanocomposite, and spinel $CoCr_2O_4$-ZrO_2 (1:3) nanocomposite.

The XRD analysis for the prepared composites confirms these findings match with the standard diffraction data for $CoCr_2O_4$ and ZrO_2[2,38]. The essential peaks of m-ZrO_2 shift toward high diffraction angle (2θ) after incorporating the crystal lattice, which indicates the formation of a metallic connection between Zr and Co in the spinal structure because both have a coordination number of six [38]. This case is an attitude to Co^{2+} and Cr^{3+} in spinel have less ionic radii compared with Zr^{4+} and equal to 0.709 Å, 0.615 Å, and 0.747 Å respectively [2,39]. On the other hand, the mean crystal sizes (L) for all samples were found using Scherer's equation [40-45]. Where k, denotes the shape constant, λ is Cu's wavelength using as a source of x-ray, 2θ is a Bragg diffraction angle, and (FWHM) is meaning a full width at half maximum intensity.

$$L = \frac{k\,\lambda}{\beta\ Cos\ \theta} \quad \ldots (6)$$

The mean crystalline diameters of the spinel $CoCr_2O_4$, ZrO_2, and the 1:2, and 1: 3 ratios spinel $CoCr_2O_4/ZrO_2$ composites were found equal to 15.5823 nm, 8.1785 nm, 9.6355 nm, and 9.0929 nm respectively. The addition of ZrO_2 in varied ratios to spinel $CoCr_2O_4$ leads to reduce the mean crystal size by elevating the ratio of ZrO_2 that will enhance the surface and optical characteristics.

B. Morphology of studied photocatalyst surfaces

1. **SEM analysis** was used to determine the morphology of the sample's surface using (FESEM FEI Nova Nano SEM 450). The SEM images of spinel $CoCr_2O_4$, ZrO_2, and their nanocomposites surfaces in Figure 3 demonstrate that the shape of the synthesized spinel $CoCr_2O_4$ is nanocrystals, which is consistent with the XRD and literature results [46]. The spinel $CoCr_2O_4$-ZrO_2 composites and ZrO_2 appear quasi-spherical shapes, that due to the high proportion of ZrO_2 in comparison to spinel $CoCr_2O_4$, which is used to increase the lightness of spinel $CoCr_2O_4$ during prepared composites, this vital step to improve their optical properties when used as a photocatalyst. ZrO_2 is a commercially available substance having a micron-scale structure because it is having a high ability to agglomerate with fine powder.

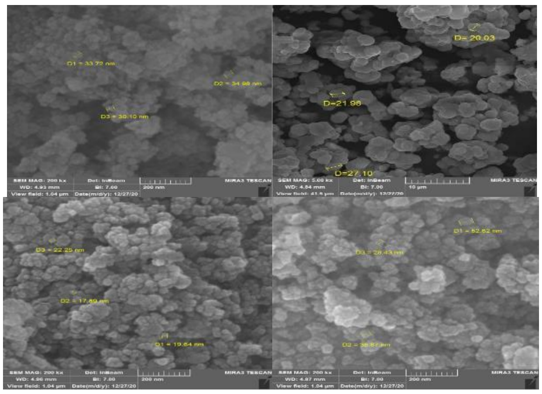

Figure 3: SEM images of spinel $CoCr_2O_4$ (a), ZrO_2 (b), a composite of spinel $CoCr_2O_4$ and ZrO_2 (1:2) (c), and a combination of spinel $CoCr_2O_4$ and ZrO_2 (1:3) (d).

EDX analysis was used to validate the sample's components. As seen in Figure 4, the spinel $CoCr_2O_4$ contains Co, Cr, and O, ZrO_2 contain Zr and O, and its composites spinel $CoCr_2O_4$-ZrO_2 also contain Co, Zr, Cr, and O, without any impurities, this is a good agreement with reported in references [19, 47].

C. Optical property of studied photocatalyst

The optical energy bandgaps (Eg in eV) were determined for all photocatalyst samples using the Tauc equation [20,48], as seen in equations 7 and 8.

$$\alpha h v = k(hv - Eg)^m \quad \dots (7)$$

$$\alpha = \frac{(2.303\, A)}{t} \quad \dots (8)$$

Where, absorption coefficient(α), Plank's constant(h), light, frequency(ν), optical constant(k), thickness(t), absorbance(A), and constant value (m) is maybe equal to 1/2 or 2 for direct (allowed) transitions and indirect (forbidden) transitions, respectively.

According to the plotted Tauc equations in Figures 5, 6, 7, and 8, the bandgap of spinel $CoCr_2O_4$ elevates with elevated the dose of ZrO_2 in spinel $CoCr_2O_4/ZrO_2$ (1:2), spinel $CoCr_2O_4/ZrO_2$ (1:3), due to ZrO_2 has a maximum bandgap (5 eV) with the direct transition. The bandgap of spinel $CoCr_2O_4$ and it's composite 1:2 and 1:3 found to be direct transition also with magnitudes equal to 3.2 eV, 4.7 eV, 4.8 eV, respectively.

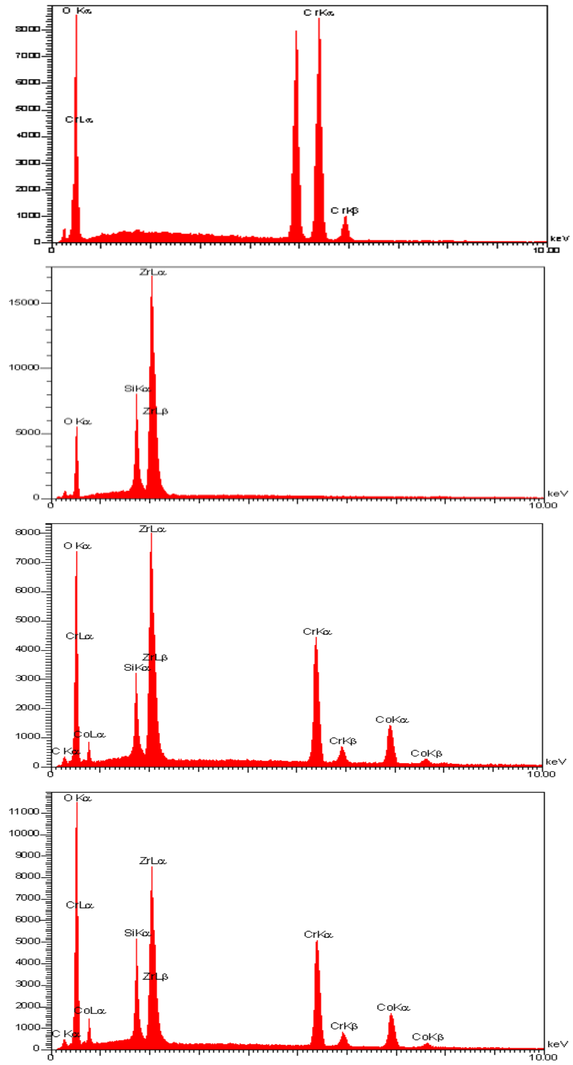

Figure 4: EDX spectra of spinel $CoCr_2O_4$(a), ZrO_2(b), spinel $CoCr_2O_4$- ZrO_2 (1:2) composite(c) and spinel $CoCr_2O_4$- ZrO_2 (1:3) composite(D)

D. Photo-decolorization of Fe(II)-(luminol-Tyrosine) dye

After determining the effectiveness of the obtained spinel $CoCr_2O_4$ nanocrystals and their nanocomposite as a spinel $CoCr_2O_4$-ZrO_2, they were applied in decolorization of Fe (II)-(luminol-Tyrosine) complex as a chocolate-colored solution that disappearance its color after irradiation for 1 h. After used composite, the apparent rate constant has elevated, and the photo-decolorization efficiency increases also from 17.57% using spinel to 30.67% and 41.97% using 1:2 and 1:3 composite ratios, respectively.

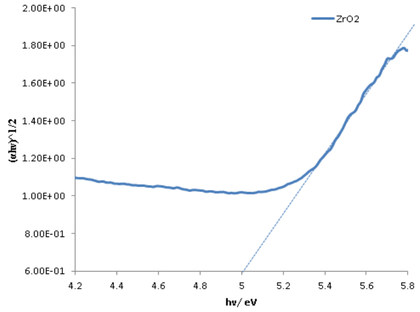

Figure 5: Tauc plot for ZrO_2 as a direct bandgap

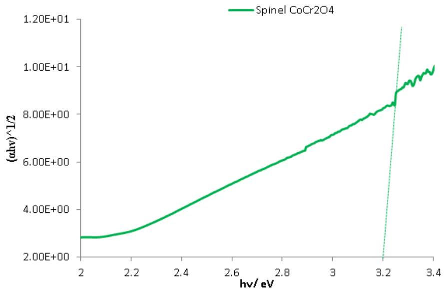

Figure 6: Tauc plot for spinel $CoCr_2O_4$ as a direct bandgap

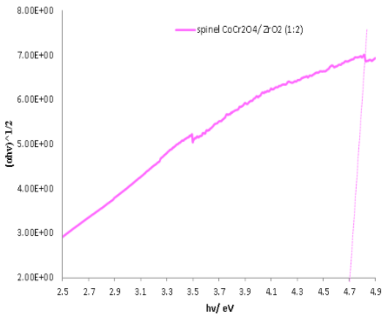

Figure 7: Tauc plot for spinel $CoCr_2O_4$/ ZrO_2 (1:2) nanocomposites as a direct bandgap

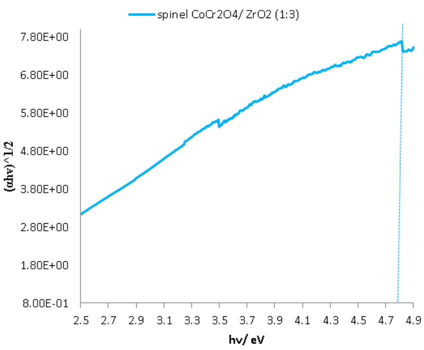

Figure 8: Tauc plot for spinel $CoCr_2O_4$/ ZrO_2 (1:3) nanocomposites as a direct bandgap

This attitude increases the lightness and acidity of spinel $CoCr_2O_4$ nanocrystals' surface through the manufacture of their composites that leads to an increase in the adsorption of hydroxyl ions [2,5]. Hence, the hydroxyl radicals will generate when the solution is exposed to UV or visible light [49-51]. Additionally, this modification surface increase the spacing of changes on the photocatalyst and the electron-hole recombination time will reduce [3,48].

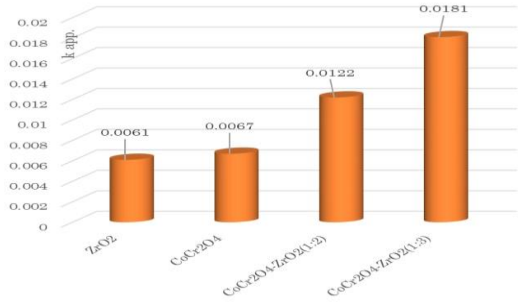

Figure 9: The relation between the apparent rate constant for Fe(II)-(luminol-Tyrosine) complex decolorization in studied photocatalyst solution

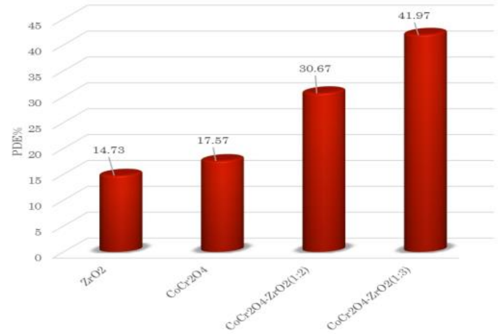

Figure 10: The relation between PDE% for Fe(II)-(luminol-Tyrosine) complex decolorization in studied photocatalyst solution

4.Conclusion

Spinel $CoCr_2O_4$ nanocrystals created using a one-step co-precipitation method. The 1:2 and 1:3 ratios of spinel$CoCr_2O_4$:ZrO_2 were successfully synthesized as nanocomposites that were accomplished using ultrasonic waves as an environmentally friendly approach. The produced photocatalysts were confirmed using XRD, SEM, and EDX measurements. Additionally, there is an optical bandgap. The XRD data suggest the production of spinel $CoCr_2O_4$ as a nanocrystalline orthorhombic phase, which agrees with miller's XRD study. SEM images and EDX spectra acquired show that the synthesis spinel $CoCr_2O_4$ is nanocrystals. Spinel $CoCr_2O_4$'s optical band gap was increased after integrating with ZrO_2 to form nano-composites. Spinel $CoCr_2O_4$'s photoreaction activity rose as well after the modification to produce the nanocomposites

5.Conflicts of interest

"There are no conflicts to declare".

7.Acknowledgments:

This study would not have been possible without the support of the University of Kerbala's faculty of science

8.References

[1] Ahmed, L. M., Bulk and Nanocatalysts Applications in Advanced Oxidation Processes, *Oxidoreductase*, IntechOpen, UK(2020).

[2] Hayawi, M. K., Kareem, M. M., and Ahmed, L. M., Synthesis of Spinel Mn_3O_4 and Spinel Mn_3O_4/ZrO_2 Nanocomposites and Using Them in Photo-Catalytic Decolorization of Fe (II)-(4, 5-Diazafluoren-9-One 11) Complex, *Periódico Tchê Química*, **17**(34), 689–699(2020).

[3] Obaid, A. J. and Ahmed, L. M., One-Step Hydrothermal Synthesis of α- MoO_3 Nano-belts with Ultrasonic Assist for incorporating TiO_2 as a NanoComposite /acceptance in *Egypt. J. Chem*., (2021).

[4] Ali, S. M. H., Alali, M. M. A. and Ahmed, L. M., Hybrid Phosphotungstic acid -Dopamine (PTA-DA) Like-flower Nanostructure Synthesis as a Furosemide Drug Delivery System and Kinetic Study of Drug Releasing /Acceptance in *Egypt. J. Chem*. (2021).

[5] Jawad, T.M., and Ahmed, L. M., Direct Ultrasonic Synthesis of WO_3/TiO_2 Nanocomposites and Applying them in the Photodecolorization ofEosin Yellow Dye, *Periódico Tchê Química*, 17(34), 621-633 (2020).

[6] Baig, N., I Kammakakam, I., and Falath, W., Nanomaterials: a review of synthesis methods, properties, recent progress, and challenges, *Mater. Adv.*, **2**, 1821-1871,(2021).

[7] Goswami, S., Manna, P. K., Bedanta, S., Dey S. K., Chakraborty M., and De D., Surface driven exchange bias in nanocrystalline $CoCr_2O_4$, *J. Phys. D. Appl. Phys.*, **53**(30), 305303 (2020).

[8] Alattar, R. A., Saleh, H. M., Al-Hilifi, J. A., and Ahmed, L. M., Influence the addition of Fe^{2+} and H_2O_2 on removal and decolorization of textile dye (dispersive yellow 42 dye), *Egypt. J. Chem.*, **63**(9), 5–6(2020).

[9] Jawad, T. M.، AL-Lami, M. R., Hasan, A. S.، Al-Hilfi, J. A., Mohammad, R. K. and Ahmed, L. M., Synergistic Effect of dark and photoreactions on the removal and photo-decolorization of azo carmosine dye (E122) as food dye using Rutile- TiO_2 suspension, /acceptance in Egyptian Journal of Chemistry, (2021).

[10] Abass, S. K., Al-Hilfi, J. A., Abbas, S. K., and Ahmed, L. M., Preparation, characterization and study the photodecolorization of mixed-ligand binuclear Co (II) complex of Schiff base by ZnO, *Indones. J. Chem.*, **20** (2) 404- 412(2020).

[11] Karam, F. F., Saeed, N. H. M., Al Yasasri, A. H., Ahmed, L. M., and Saleh, H., Kinetic Study for Reduced the Toxicity of Textile Dyes (Reactive yellow 14 dye and Reactive green dye) Using UV-A light/ZnO System, *Egypt. J. Chem.*, **63**(8), 5–8(2020).

[12] Marhoon, A. A., Saeed, S. I., and Ahmed, L. M., Application of some effects on the Degradation of the aqueous solution of Fuchsine dye by photolysis, *J. Glob. Pharma Technol.*, **11**(9), 76–81(2019).

[13] Apostolova, I. N., Apostolov, A. T., and Wesselinowa, J. M., Multiferroic and phonon properties of pure and ion doped $CoCr_2O_4$-Bulk and nanoparticles, *J. Alloys Compd.*, **852**, 156885(2021).

[14] Mohanty, P., Sheppard, C. J., and Prinsloo, A. R. E., Field induced magnetic properties of Ni doped $CoCr_2O_4$, *AIP Conference Proceedings*, **2115**(1), 30195(2019).

[15] Chamyani, S., Salehirad, A., Oroujzadeh, N., and Fateh, D. S., Effect of fuel type on structural and physicochemical properties of solution combustion synthesized $CoCr_2O_4$ ceramic pigment nanoparticles, *Ceram. Int.*, **44**(7), 7754–7760(2018).

[16] Nadeem, K., Rehman, H. U., Zeb, F., Ali E., Kamran, M., Noshahi, N.A. and Abbas, H. Magnetic phase diagram and dielectric properties of Mn doped $CoCr_2O_4$ nanoparticles, *J. Alloys Compd.*, **832**, 155031(2020).

[17] Rasool R. Z., Nadeem K., Kamran M., Zeb F., Ahmad N., and Mumtaz M., Comparison of anomalous magnetic properties of non-collinear $CoCr_2O_4$ and NiCr2O4 nanoparticles, *J. Magn. Magn. Mater.*, **514**, 167225(2020).

[18] Manjunatha, K.., Angadi, V. J., Ribeiro, R. A. P., Oliveira, M. C., de Lázaro, S. R., Bomio, M. R. D., Matteppanavar, S., Rayaprol, S., Babu, P. D. and Pasha, U. M., Structural, electronic and magnetic properties of Sc^{3+} doped $CoCr_2O_4$ nanoparticles, *New J. Chem.*, **44**(33), 14246–14255(2020).

[19] Choudhary, P., Saxena, P., Yadav, A., Rai, V. N., and Mishra, A., Dielectric and ferroelectric properties of $CoCr_2O_4$ nanoceramics, *J. Adv. Dielectr.*, **9**(03), 1950015(2019).

[20] Jawad, T. M. and Ahmed, L. M., Synthesis of WO_3/TiO_2 nanocomposites for Use as Photocatalysts for Eosin Yellow Dye Degradation, *IOP Conference Series: Materials Science and Engineering*, **1067**(1), 12153(2021).

[21] Saeed, S. I., Attol, D. H., Eesa, M. T. and Ahmed, L. M., Zinc Oxide- Mediated Removal and Photocatalytic Treatment of Direct Orange 39 Dye as a Textile Dye/acceptance in *AIP Conference* Proceedings,(2021).

[22] Mashkour, M. S., Al-Kaim, A. F., Ahmed, L. M., and Hussein, F. H., Zinc Oxide Assisted Photocatalytic Decolorization of Reactive Red 2 Dye, *Int. J. Chem. Sci*., **9**(3), 969-979, (2011).

[23] Kzar, K. O., Mohammed, Z.F., Saeed, S.I., Ahmed, L.M., Kareem, D.I., Hadyi, H. and Kadhim, A.J. Heterogeneous photo-decolourization of cobaltous phthalocyaninate dye (Reactive green dye) catalyzed by ZnO, *AIP Conference Proceedings*, **2144**(1), 20004(2019).

[24] Ahmed, L. M., Jassim, M. A., Mohammed, M. Q., and Hamza, D. T., Advanced oxidation processes for carmoisine (E122) dye in UVA/ZnO system: Influencing pH, temperature and oxidant agents on dye solution, *Journal of Global Pharma Technology*, **10**(7), 248-254,(2018).

[25] Ahmed, L. M., Photo-Decolourization Kinetics of Acid Red 87 Dye in ZnO Suspension Under Different Types of UV-A Light, *Asian J. Chem*., **30** (9), 2134 - 2140 (2018).

[26] Jaafar, M. T., and Ahmed, L. M., Reduced the toxicity of acid black (nigrosine) dye by removal and photocatalytic activity of TiO2 and studying the effect of pH, temperatue, and the oxidant agents, *AIP Conference Proceedings*, **2290** (1), 30034(2020).

[27] Hussain, Z. A., Fakhri, F. H., Alesary, H. F., and Ahmed, L. M., ZnO Based Material as Photocatalyst for Treating the Textile Anthraquinone Derivative Dye (Dispersive Blue 26 Dye): Removal and Photocatalytic Treatment, *Journal of Physics: Conference Series*, **1664**(1), 12064(2020).

[28] Jasim, K. M. and Ahmed, L. M., TiO_2 nanoparticles sensitized by safranine O dye using UV-A light system, *IOP Conference series: Materials science and Engineering*, **571**(1),12064(2019).

[29] Ahmed, L. M., Saaed, S. I., and Marhoon, A., Effect of Oxidation Agents on Photo-Decolorization of Vitamin B12 in the Presence of ZnO/UV-A System, *Indones. J. Chem.* **18**(2). 272- 278(2018).

[30] Hussein, Z. A., Abbas, S. K. and Ahmed, L. M. UV-A activated ZrO_2 via photodecolorization of methyl green dye, *In IOP Conf. Ser.: Mater. Sci. Eng .*, **454**, 1-11(2018).

[31] Zuafuani, S. I., and Ahmed, L. M., Photocatalytic decolourization of direct orange Dye by zinc oxide under UV irradiation, *Int. J. Chem. Sci*, **13**(1), 187-196(2015).

[32] Abbas, S. K., Hassan, Z. M. and Ahmed , L. M. Influencing the Artificial UV-A light on decolorization of Chlorazol black BH Dye via using bulk ZnO Suspensions, *Journal of Physics: Conference Series***,** *IOP Publishing*, **1294**(5), 1-8(2019).

[33] Saeed, S. I., Taresh, B. H., Ahmed, L. M., Haboob, Z. F., Hassan, S. A. and Al-amir, A. A., Insight into the Oxidant Agents Effect of Removal and Photo-decolorization of Vitamin B12 Solution in Drug Tablets using ZrO_2/Acceptance in *Journal of Chemical Health Risks (JCHR)* (2021).

[34] Eesa, M.T., Juda, A. M. and Ahmed, L. M., Kinetic and Thermodynamic Study of the Photocatalytic Decolourization of Light Green SF Yellowish (Acid Green 5) Dye using Commercial Bulk Titania and Commercial Nanotitania, *International Journal of Science and Research (IJSR)*, **5**(11) 1495-1500(2016).

[35] Tian, Z., Zhu, C., Wang, J., Xia, Z., Liu, Y., and Yuan, S., Size dependence of structure and magnetic properties of $CoCr_2O_4$ nanoparticles synthesized by hydrothermal technique, *J. Magn. Magn. Mater.*, **377**, 176–182, (2015).

[36] Choudhary, P., Yadav, A., and Varshney, D., Structural and optical studies of nanocrystalline $ZnCr_2O_4$ and $CoCr_2O_4$ spinel, *AIP Conference Proceedings*, **1832** (1), 50051(2017).

[37] Betancur-Granados, N. and Restrepo-Baena, O. J., Flame spray pyrolysis synthesis of ceramic nanopigments $CoCr_2O_4$: The effect of key variables, *J. Eur. Ceram. Soc.*, **37**(15), 5051–5056(2017).

[38] Kassem, M. A., El-Fadl, A. A., Nashaat, A. M., and Nakamura, H., Structure, optical and varying magnetic properties of insulating MCr_2O_4 (M= Co, Zn, Mg and Cd) nanospinels, *J. Alloys Compd.,*. **790**, 853–862(2019).

[39] Ghosh, D. C., and Biswas, R., Theoretical Calculation of Absolute Radii of Atoms and Ions. Part 2. The Ionic Radii, *Int. J. Mol. Sci*., **4**(6), 379-407(2003).

[40] Fadhil, E. S., Ahmed, L. M. and Mohammed, A. F., Effect of Silver Doping On Structural and Photocatalytic Circumstances of ZnO Nanoparticles, *Iraqi Journal of Nanotechnology, synthesis and application* **1**, 13-20(2020).

[41] Ahmed, L. M., Hussein, F. H. and Mahdi, A. . Photocatalytic Dehydrogenation of Aqueous Methanol Solution by Naked and Platinized TiO2 Nanoparticles, *Asian Journal of Chemistry*. **24**(12). 5564-5568(2012).

[42] Ahmed, L. M., Ivanova, I., Hussein, F. H. and Bahnemann, D. W., Role of Platinum Deposited on TiO2 in Photocatalytic Methanol Oxidation and Dehydrogenation Reactions, *International Journal of Photoenergy*, 1-9 (2014).

[43] Al-Shakban, M, Abbas, A. M., Ahmed, L. M., Chemical Vapour Deposition of CdS Thin Films at Low Temperatures from Cadmium Ethyl Xanthate, *Egyptian Journal of Chemistry*, **64**(5), 2533 - 2538, (2021).

[44]Mohammed, B. A., and Ahmed, L. M., Improvement the Photo Catalytic Properties of ZnS nanoparticle with Loaded Manganese and Chromium by Co-Precipitation Method, *Journal of Global Pharma Technology*, **10**(7), 129- 138, (2018).

[45] Ali, S. M. H., Alali, M. M. M. A. and Ahmed, L. M., Flower-like Hierarchical Nanostructures Synthesis of Polyoxometalate- Dopamine and loading Furosemide on its surface and aging them using microwave technique/Acceptance in *AIP Conference Proceedings* (2021).

[46] Dai,Y., Wang, H., Liu, S., Smith, K. J., Wolf, M. O., and MacLachlan, M. J., $CoCr_2O_4$ nanospheres for low temperature methane oxidation, *Cryst. Eng. Comm*, **22**(26), 4404–4415(2020).

[47] Moudood, M. A., Sabur, A., Lutfi, A., Ali, M. Y., and Jaafar, I. H., Investigation of The Machinability of Non-Conductive ZrO_2 With Different Tool Electrodes in Edm., *Int. J. Automot. Mech. Eng.*, **10**, 1866-1876(2014).

[48] Fakhri, F. H. and Ahmed, L. M., Incorporation Cds with Zns as Composite and Using in Photo-Decolorization of Congo Red Dye, *Indones. J. Chem.*, **19**(4), 936-943, 2019.

[49] Ahmed L.M., Abd-Kadium E. Q., Salman R. A., Wali H. K. and Nasser N. K., Photocatalytic decolorization of dispersive yellow 42 dye in ZnO/UV-A System, *Iraqi National Journal of Chemistry*, **17** (4), 198-209(2017).

[50] Alattar R. A., Hassan Z. M., Abass S. K., and Ahmad L. M., Synthesis, characterization and study the

photodecolorization of Schiff base Fe (III) complex in ZnO/Uv-A light system, *AIP Conference Proceedings*, **2290**(1), 30032(2020).

[51] Ahmed L. M., Tawfeeq F. T., Abed Al-Ameer M. H., Al-Hussein K. A.,Athaab A. R., Photo-Degradation of Reactive Yellow 14 Dye(A Textile Dye) Employing ZnO as Photocatalyst, *Journal of Geoscience and Environment Protection*, **4**, 34-44(2016).